Research Article

MOLECULAR PAIN

Molecular Pain
Volume 15: 1–16

DOI: 10.1177/1744806919845750
journals.sagepub.com/home/mpx
SAGE

Tachykinins modulate nociceptive responsiveness and sensitization: In vivo electrical characterization of primary sensory neurons in tachykinin knockout (Tac1 KO) mice

Silvia Gutierrez[1], P Abigail Alvarado-Vázquez[1], James C Eisenach[1], E Alfonso Romero-Sandoval[1], and M Danilo Boada[1]

Abstract

Since the failure of specific substance P antagonists to induce analgesia, the role of tachykinins in the development of neuropathic pain states has been discounted. This conclusion was reached without studies on the role of tachykinins in normal patterns of primary afferents response and sensitization or the consequences of their absence on the modulation of primary mechanonociceptive afferents after injury. Nociceptive afferents from animals lacking tachykinins (Tac1 knockout) showed a disrupted pattern of activation to tonic suprathreshold mechanical stimulation. These nociceptors failed to encode the duration and magnitude of natural pronociceptive stimuli or to develop mechanical sensitization as consequence of this stimulation. Moreover, paw edema, hypersensitivity, and weight bearing were also reduced in Tac1 knockout mice 24 h after paw incision surgery. At this time, nociceptive afferents from these animals did not show the normal sensitization to mechanical stimulation or altered membrane electrical hyperexcitability as observed in wild-type animals. These changes occurred despite a similar increase in calcitonin gene-related peptide immunoreactivity in sensory neurons in Tac1 knockout and normal mice. Based on these observations, we conclude that tachykinins are critical modulators of primary nociceptive afferents, with a preeminent role in the electrical control of their excitability with sustained activation or injury.

Keywords

Neuropeptides, nociception, sensitization, tachykinin knockout, incision, substance P, calcitonin gene-related peptide, transient receptor potential cation channel vanilloid 1

Date Received: 23 February 2019; revised: 21 March 2019; accepted: 22 March 2019

Introduction

Tachykinin peptides participate in numerous important physiological processes in nervous, immune, and respiratory systems, among others. In the somatosensory system, the tachykinins substance P (SP), neurokinin A, neuropeptide K, and neuropeptide Y are all encoded by the Tac1 gene and are synthetized by C and Aδ nociceptive primary sensory neurons projecting to nociceptive and nonnociceptive specific laminae of the spinal dorsal horn.[1–3]

A disruption in tachykinin signaling results in a diminished nociceptive behavioral response evoked by mild mechanical stimulation in different pain models in mice lacking the preprotachykinin A gene (termed Tac1 knockout (Tac1 KO))[4–6] and those lacking neurokinin-1 receptors.[7] However, the precise function of these tachykinins in the modulation of nociceptive afferent function and signaling remains unclear.

[1]Wake Forest Baptist Medical Center, Winston-Salem, NC, USA

Corresponding Author:
M Danilo Boada, Wake Forest Baptist Medical Center, 1 Medical Center Blvd., Winston-Salem, NC 27103, USA.
Email: mboada@wakehealth.edu

These seminal studies proposed that tachykinins act through their central[7] release in the superficial laminae of the spinal cord, ultimately inducing central sensitization.[8–10] Later studies showed that these tachykinins also trigger local release of pro-inflammatory factors[11,12] that induce plasma extravasation (neurogenic inflammation[13]) and ultimately peripheral sensitization. This study focuses on an alternative hypothesis that tachykinins directly modulate the nociceptive encoding functions of peripheral sensory neurons, resulting in the enhanced responsiveness observed in primary neuronal sensitization. To test this hypothesis, we study the response patterns of sensory afferents in Tac1 KO and wild-type (WT) mice using two models: first, in vivo intracellular recordings in dorsal root ganglia (DRG) neurons in naive animals before, during, and after intensity- and duration-controlled suprathreshold mechanical stimulation; and second, similar electrophysiological studies 24 h after a paw incision.

Since a thorough direct functional characterization of peripheral sensory neurons in relation to nociceptive behaviors has not been done in Tac1 KO (vs. WT), we have compared behavioral (hypersensitivity) and edema (paw circumference) responses in WT and Tac1 KO mice before and after paw incision. Then, we assessed the proportion of sensory neuron subtypes, their passive and active electrical properties, and their mechanical threshold in WT and Tac1 KO naive mice, and those after paw incision. Since other factors such as calcitonin gene-related peptide (CGRP) or the transient receptor potential cation channel vanilloid 1 (TRPV1) influence the development of peripheral sensitization,[14–16] we also characterized the changes in immunoreactivity of these in DRG neurons in which they were expressed or co-expressed in our models. This characterization allowed us to determine the type of changes that occur following peripheral sensitization and how lack of tachykinins altered responses to paw incision. These studies guided our studies using the second model to directly test our hypothesis. Importantly, some reports indicate that TRPV1-positive neurons colocalized with CGRP, SP, as well as IB4 in both trigeminal and DRG neurons in the rat.[17] However, in mice, this receptor has been show nonrelated to the IB4-binding population and more widely distributed along both CGRP- and SP-positive neurons.[18]

From a responsiveness stand point, the activation of nociceptive afferents leads to the generation of action potentials (APs) and the release of neuropeptides from multiple areas (at least at peripheral and central nerve endings).[19–21] In this context, it appears only logical to question if the absence of these neuropeptides modulates the response patterns of nociceptive afferents prior to confounding effects (e.g., inflammation, tissue injury). Unfortunately, since the development of viable tachykinin knockout mice (B6.Cg-*Tac1*^{tm1Bbm}/J),[5] no detailed electrophysiological study has examined the potential modulatory effects of neurokinins in the patterns of responsiveness of peripheral afferents.

This study aims to fill this gap in our knowledge and to clarify whether the absence of these tachykinins alters the manner that nociceptive and nonnociceptive afferents react to acute peripheral tissue damage (paw incision). Furthermore, we study the patterns of activation of mechanosensitive afferents to controlled stimulation and their sensitization in the absence of tachykinin neuropeptides.

Methods

Animals

Sixteen male mice (eight C57BL/6J (WT) and eight B6.Cg-*Tac1*^{tm1Bbm}/J (Tac1 KO)), four to six weeks of age, were used (The Jackson Laboratory, Bar Harbor, ME, USA). Eight animals, four of each breed, were studied in protocols examining the *normal* patterns of response to mechanical stimulation and sensitization of different subtypes of nociceptive and nonnociceptive primary sensory neurons. Eight other animals, four of each breed, were studied in protocols to determine the effect of *paw incision* on mechanical sensitivity. Animals were housed in pairs, in a climate-controlled room under a 12-h light/dark cycle. The use and handling of animals were in accordance with guidelines provided by the National Institutes of Health and the International Association for the Study of Pain, and all procedures and experiments were approved by the Institutional Animal Care and Use Committee of Wake Forest University Health Sciences.

Electrophysiology

Animals in both experimental groups (normal and with paw incision) were deeply anesthetized with isoflurane 3% (Teva Pharmaceuticals, North Wales, PA, USA). The trachea was intubated, and the lungs ventilated using pressure-controlled ventilation (Inspira PCV, Harvard Apparatus, Holliston, MA, USA) with humidified oxygen. Heart rate and noninvasive blood pressure were monitored throughout as a guide to depth of anesthesia. Inspired end tidal isoflurane concentration was maintained at 2% throughout the study. A dorsal incision was made in the thoraco-lumbar midline, and the L4 DRG and adjacent spinal cord were exposed by laminectomy as described previously (Figure 1(a)).[22] The tissue was continuously superfused with oxygenated artificial cerebrospinal fluid ((in mM): 127.0 NaCl, 1.9 KCl, 1.2 KH_2PO_4, 1.3 $MgSO_4$, 2.4 $CaCl_2$, 26.0 $NaHCO_3$, and 10.0 D-glucose). The spinal column was secured using

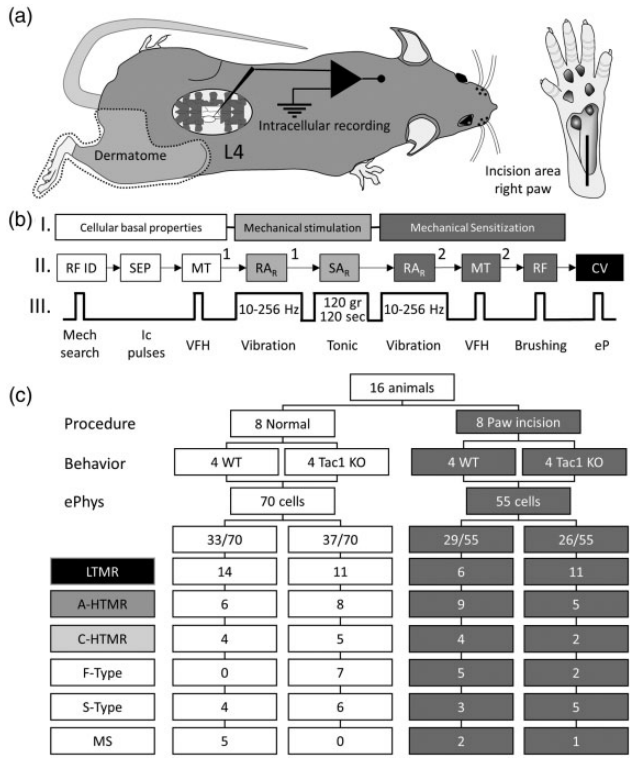

Figure 1. (a) Schematic diagram of the L4 intracellular recording from neurons in the L4 dorsal root ganglia, the area of search for the cellular RF in its dermatome (light gray area) and the region on the ipsilateral paw were the incision was performed (right diagram). (b) Explanative diagram of the stages used in the current protocol (B_I), the physiological parameter evaluated in every stage (B_{II}), and the applied stimuli (B_{III}) (*cellular basal properties* (white box), B_{II}: receptor field identification (RF ID), somatic electrical properties (SEPs), normal mechanical threshold (MT^1); *controlled mechanical stimulation* (light gray box), B_{II}: normal rapid adaptative response $\left(RA\frac{I}{R}\right)$ and normal slow adaptative response (SA_R), mechanical); and *mechanical sensitization* (dark gray box), BII: sensitized rapid adaptative responses $\left(RA\frac{I}{R}\right)$ and sensitized mechanical threshold (MT^2)) and the stimuli used in every case (B_{III}) indicated by the squared trace (Ic pulses: injected current pulses; VFH: Von frey hair; eP: peripheral electrical stimulation pulse; CV: conduction velocity). (c) Flowchart, procedures and classification of the neurons included in the study in WT (C57BL/6J) and Tac1 KO (B6.*Cg-Tac1*^{tm1Bbm}/J), per cellular subtype: (LTMR: low-threshold mechanoreceptors; A-HTMR: A-fiber high-threshold mechanoreceptor (AHTMR); C-HTMR: C-fiber high-threshold mechanoreceptor (CHTMR); F-type: fast AP dynamic mechanically unresponsive; S-type: slow AP dynamics mechanically unresponsive; MS: muscular spindle).

custom clamps, and the preparation was transferred to a preheated (32°C–34°C) recording chamber where the superfusate temperature was slowly raised to 37°C ± 0.2°C using an infusion pump (MPRE8; Cell MicroControls, Norfolk, VA, USA). Pool temperature adjacent to the DRG was monitored with a thermocouple (IT-23; Physitemp, Clifton, NJ, USA). Rectal temperature (RET-3; Physitemp) was maintained at 34°C ± 1°C with radiant heat.

The electrophysiological recordings from each animal were limited to a maximum duration of 75 min in order to diminish the likelihood that experimental manipulation would result in sensitization. DRG neuronal somata were impaled with quartz micropipettes (80–250 MΩ) containing 1M potassium acetate. Direct current output from an Axoclamp 2B amplifier (Axon Instruments/Molecular Devices, Sunnyvale, CA, USA) was digitized and analyzed off-line using Spike2 (CED, Cambridge, UK). Sampling rate for intracellular recordings was 21 kHz throughout (MicroPower1401; CED).

Cellular classification protocol

Although the general procedure to classify primary sensory afferents was applied as described in Boada et al.,[23] the receptor field (RF) search procedure was modified to always begin at the center of the animal's right paw in a concentric pattern (to first cover the glabrous skin of the paw and then extended to the hairy skin of the limb), 20 mm below the skin midline surgical wounded area (animal's back). RFs were located with the aid of a stereomicroscope using increasing mechanical stimulation; the latter progressed from light touch with a fine sable hair paintbrush to searching with blunt probe (back of the paintbrush) and ultimately gentle to strong pinch with fine-tipped forceps. Based on the combination of their mechanical threshold, conduction velocity (CV) and dynamic response (phasic: on–off; tonic) neurons were classified into three groups: LTMRs (low-threshold mechanoreceptors), AHTMRs (A-fiber high-threshold mechanoreceptors), and C-fiber high-threshold mechanoreceptors (CHTMRs). Specific cellular subtypes such as slowly adapting (SA) tactile afferent neurons (SAI and SAII), C-polymodal nociceptor (nociceptors that saturate their responses well below the mechanical nociceptive thresholds in human)[24–27] and nonelectrically excitable cells were excluded from this study.

Cells that were electrically excitable but without mechanical RF were separated in two different populations based on the shape of the AP:[23,28–30] neurons with inflection in the repolarizing phase (S-type neurons) and neurons without this inflection (F-type neurons). To more clearly determine the presence of this inflection, the differentiated records of the AP were used (presence or absence of a second additional negative component in the time course of the AP derivative). Since RF properties, especially response characteristics, were used to define differences in the fast-conducting afferents (those without inflected APs), the ability to accurately define and categorize these two populations further was not possible. After electrical characterization, nonperipherally excitable afferent and afferents identified as

muscular spindles were noted to be included in the distribution but not otherwise examined.

All included cells satisfied the following requirements: resting membrane potential (Em) more negative than −40 mV, AP amplitude ≥30 mV, and the presence of after hyperpolarization (AHP). Passive membrane properties indicative of poor impalement (extremely low input resistance (Ri) and/or extremely short time constant (tau, τ)) were also reasons for exclusion. Fiber CV was always measured at the end of the recording.

Mechanical sensitivity and cellular excitability

Peripheral and somatic cellular excitability were measured at three stages (Figure 1(b)): (1) cellular basal properties, (2) controlled mechanical stimulation, and (3) mechanical sensitization.

1. Cellular basal properties: This protocol applied to both groups (normal and paw incision) and included: Cell and RF characterization, somatic electrical properties (SEPs), and afferent CV.
   a. Cell and RF characterization (RF identification): After identifying the cellular RF area of responsiveness to the search stimulus, the area was marked using a red fine point marker. This initial procedure was performed in a gentle manner to avoid damaging the skin (as assessed visually by lack of development of erythema, edema, glossiness, etc.).
   b. SEPs: Active membrane properties of all excitable neurons were analyzed in APs obtained during RF characterization. These parameters included amplitude and duration of the AP and AHP of the AP, along with the maximum rates of spike depolarization and repolarization; AP and AHP durations were measured at half amplitude (D50 and AHP50, respectively) to minimize hyperpolarization-related artifacts. Passive properties analyzed were Em, Ri, Tau, and where possible, rheobase; all but the latter were determined by injecting incremental hyperpolarizing current pulses (Ic pulses: ≤0.1 nA, 500 ms) through balanced electrodes.
   c. Mechanical thresholds (Figure 1(b), MT^1) were determined with calibrated von Frey filaments (Stoelting, Wood Dale, IL, USA), activating the most sensitive area of the cellular RF. Postdischarge hyperpolarization (PDH)[31] was evaluated during this procedure (paw incision) and during controlled mechanical stimulation (control) after and before tonic stimulation (see below).
   d. CV. Because intact lumbar DRGs serve multiple nerves, spike latency was obtained by stimulating the RF at the skin surface using a bipolar electrode (0.5 Hz, current range: 0.1–1.2 mA) and a stimulus isolator (A360LA; WPI, Sarasota, FL, USA); this was performed following all-natural stimulation to prevent potential alterations in RF properties by electrical stimulation. All measurements were obtained using the absolute minimum intensity required to excite neurons consistently without jitter; this variability (jitter) in the AP generation latency (particularly at significantly shorter latencies) seen at traditional (i.e., two- to three-fold threshold) intensity has been presumed to reflect spread to more proximal sites along axons. Stimuli ranged in duration from 50 to 100 μs; utilization time was not taken into account. Conduction distances were measured for each afferent on termination of the experiment by inserting a pin through the RF (marked with ink at the time of recording) and carefully measuring the distance to the DRG along the closest nerve.
2. Controlled mechanical stimulation. This procedure was applied only to normal animals and included vibratory stimulation and tonic stimulation.
   a. Vibratory stimulation. Cellular rapid adaptative response (RA_R) was evaluated by applying rapid nonnociceptive mechanical stimulation (vibration) directly on the most sensitive area of the cellular RF. For this purpose, we used either a tuning fork (256 Hz) (LTMR and HTMR) or vibration pulses (HTMR): Pulses of 500 ms (inner cycle: 10-100 Hz) at 2 Hz were delivered by a 1-mm hollow crystal probe (0.2 gr) attached to an 8-ohm speaker and controlled by a pulse generator (Grass S44 stimulator; Grass Instruments, West Warwick, RI, USA) connected to a function generator (Wavetek 188-S-1257, San Diego, CA, USA). The probe tip was flamed and polished to eliminate skin damage and its offset set to maintain contact with the skin during the stimulation. Maximum tip displacement during the stimulation at 10 Hz using squared pulses was ∼0.25 mm. Both cellular initial responsiveness (1:1) and habituation patterns to this stimulation were evaluated (Figure 1(b), RA_R^1).
   b. Tonic stimulation. Cellular slow adaptative response (SA_R) was evaluated by applying tonic calibrated mechanical stimulation directly on the most sensitive area of the cellular RF. A calibrated clamp (120 gf, 0.12 N) (TKL-1-120, AROSurgical, Newport Beach, CA, USA) was applied by hand in a steady motion perpendicular to the cellular RF (90°). The clamp surface was previously marked to ensure only to clamp 1.5 mm^2 of skin. This stimulus was applied with different durations and patterns depending on the

cellular identity. LTMRs: 3 consecutive applications, 10 s each separated by 10 s. HTMRs: 1 application, 120 s. Several properties were analyzed: response duration (s), maximal instantaneous frequency (IFmax) (Hz), adaptation rate (phasic or tonic), and response dynamics: *Rising phase* (RP) between the first cellular activation until it reached the IFmax, *falling phase* (FP) between IFmax to its 10% of the maximum IF ($IF_{10\%}$)), and response *plateau* from $IF_{10\%}$ to the end of the response. These phases were evaluated independently in every afferent in terms of the number of APs per phase, the time per phase, the mean IF (IFmean) (±standard error (SE)), and the slope of change in AP frequency during each phase. AP electrical characteristics and membrane potential values were analyzed at the beginning and end of the cellular tonic activation (Figure 1(b), SA_R)

3. Mechanical sensitization: After tonic mechanical stimulation, the response to vibratory stimulation (Figure 1(b), RA_R^2) and the afferent mechanical threshold (Figure 1(b), MT^2) and response to brushing were retested and compared with data obtained earlier for that afferent.

Incision

One week after arrival baseline paw withdrawal threshold was determined, and paw incision surgery was performed as described previously.[32] Briefly, mice were anesthetized with isoflurane in oxygen (3% induction, 1.5%–2% maintenance), the right hind paw was aseptically cleaned with 10% povidone-iodine solution, then a 5-mm longitudinal incision was made in the plantar aspect of the paw approximately 5 mm from the edge of the heel using a No. 11 scalpel. The adjacent muscle and ligaments were elevated for 6–8 s using curved forceps. The surgery was carried out under sterile conditions. The incision was closed using 5-0 nylon mattress sutures.

Paw edema

Paw edema was determined by measuring the circumference of the paw before the surgery and at the beginning and end of each behavioral evaluation, as described previously.[33] Mice were briefly anesthetized with 1.5%–2% isoflurane in oxygen, and the circumference of the right and left paws was measured using a 4-0 silk thread that was placed around the center of the incision. The length of the thread was then measured using a calibrated caliper.

Behavioral tests

Behavioral assessments were performed before 24 h after paw incision. For mechanical withdrawal threshold assessment, mice were placed on a mesh floor in a plastic cage and acclimatized to the environment for at least three consecutive days before surgery and for 30 min prior to testing. Paw withdrawal threshold was determined by applying calibrated von Frey filaments (Stoeling, Wood Dale, IL, USA) to the plantar aspect of the paw and lateral to the incision. We used the up–down statistical method as described previously.[33] A positive response was noted when the animal rapidly withdrew the paw or when flinching was observed after the stimulation.

For static weight bearing, we utilized the incapacitance test using an incapacitance meter apparatus (Stoelting, IL, version 5.64). Mice were habituated to the apparatus at least three consecutive days before surgery. The apparatus consists of two calibrated weight plates that measured the weight that the animal distributed between hind paws. Mice were placed on top of the calibrated weight plates, and at least six measurements of their body weight were taken every 3 s. The ratio of body weight distribution was calculated by dividing the averaged value of the paw ipsilateral to surgery by the value of the contralateral paw. The baseline values of noninjured animals were similar or equal to 1. A ratio less than 1 indicates that the animal distributed their weight on the noninjured limb. All behavioral measurements were performed by an observer who was blinded to genotype.

Immunocytochemistry

Tissue preparation. Follow the electrophysiological experiments, the thorax was opened, and fixative (4% paraformaldehyde in 0.1 M phosphate buffer, pH 7.4) was perfused through the left ventricle with a peristaltic pump at 20 ml/min for 15 min. Ipsilateral L4 DRGs were then identified, removed, and immersed in fixative for 2 h at 4°C. Afterward, ganglia were washed 0.01M phosphate-buffered saline (PBS) and immersed in 30% sucrose at 4°C for cryoprotection until sectioned on a cryostat. Sections (18 μm) were collected on slides and stored at −80°C until processed. Sections from three animals per group were processed simultaneously and antibodies for SP, CGRP and TRPV1 carboxy terminus were used. Sections were washed with PBS with 0.1% Triton X-100 (PBST), incubated 1 h in blocking solution (1.5% normal donkey serum (#017–000-121; Jackson Immuno Research Labs, West grove, PA, USA) in PBST and overnight at 4°C with the following primary antibodies: rat anti-SP (1:500, #556312; BD Biosciences, San Jose, CA, USA), rabbit anti-CGRP (1:10 000, #C8198; Sigma, St. Louis, MO, USA), and guinea pig

antivanilloid receptor 1 (1:1000, #GP14100; Neuromics, Edina, MN, USA). Afterward, sections were washed three times for 10 min with PBS and incubated 2 h at room temperature with the corresponding secondary antibodies: donkey antirat cyanine 2 (1:400), antirabbit cyanine 3 (1:500), and antiguinea pig cyanine 5 (1:500) (Jackson Immuno Research Labs, West Grove, PA, USA). Finally, sections were washed thoroughly in PBS, mounted on plus-slides, air-dried, dehydrated in ethanol, cleared in xylene, and cover slipped with DPX mounting media (a mixture of distyrene, a plasticizer, and xylene used as a synthetic resin mounting media).

TRPV1 antibody specificity was tested using a blocking peptide following the manufacturer's instructions (#P14100; Neuromics, Northfield, MN, USA). There is not a commercially available blocking peptide for rabbit anti-CGRP (#C8198; Sigma, St. Louis, MO, USA) although this antibody is being previously used in mouse tissue.[34] TRPV1, SP, and CGRP antibody specificity were also verified by deletion of the primary antibody (data not shown).

Image acquisition and analysis

Images from three to five randomly selected sections were captured with a CCD digital camera attached to a Nikon E600 epifluorescence microscope with a 20× objective. Images obtained were coded so the experimenter performing image analysis was blinded to group. Images were quantified using Image J (U.S. National Institutes of Health, Bethesda, MD, USA, http://imagej.nih.gov/ij/,997–2011). Cells were randomly selected using a macro for a cross grid (grid size = 4900 μm^2). They were selected for further analysis if they were positive for the marker (SP or CGRP) and if their boundaries overlap with any cross in the grid. Once selected, the area of these neurons was outlined manually through cell body boundaries and the intensity of immunostaining to SP or CGRP was quantified automatically in pixels. An adjacent area to the cells was used to define the background to be subtracted from each measurement. The number of pixels was then divided to each neuron area, and the average was calculated per animal and per group. These positive cells for SP or CGRP were qualitatively analyzed to define whether they were also immunoreactive to the other markers (double and/or triple positive).

Statistical analysis

Prior to analysis, parametric assumptions were evaluated for all variables using histograms, identification of outliers with boxplots, descriptive statistics, and the Shapiro–Wilk test for normality. Data are reported as medians (range) if not normally distributed or means (SE) if normally distributed. Student's t test and repeated measures analysis of variance (ANOVA) were used for normally distributed data, and Friedman test and Mann–Whitney U test were used for not normally distributed data. Changes in Em in AHTMR over time were analyzed using repeated measures ANOVA with Greenhouse and Geisser sphericity correction as distributions at each time point proved to be parametric, and there were no significant outliers. Friedman tests were run on number of APs per stimuli and duration data as the distributions were nonparametric at one or more time points in each dependent variable. For all analyses, p was set at 0.05 for statistical significance. All post hoc analyses were Bonferroni adjusted. Analyses were carried out using SPSS Statistics for Windows, version 22 (IBM Corp., Armonk, NY, USA) and Origin 9.5 (Northampton, MA, USA).

Results

Intracellular recordings were obtained in 125 sensory neurons innervating the L4 dermatome from 16 animals. The distribution of cell classifications in WT and Tac1 KO under normal conditions and 24 h after surgery is shown in Figure 1(c). Of note, approximately one-third of cells were LTMRs, approximately one-fourth were AHTMRs, and approximately one-tenth were CHTMRs with no significant difference between WT and Tac1 KO in either normal or incision groups.

Normal animals

Baseline mechanical thresholds (MT^1) and vibratory stimulation. All LTMR afferents collected from both breeds followed the 256 Hz tuning fork (TF) and 10 Hz vibration application with fidelity, responded to brushing and had similar MT^1 (WT: 0.07 mN (range 0.07–0.7 mN) vs. Tac1 KO: 0.19 mN (range: 0.07–0.7 mN)). Conversely, none of the HTMR afferents in both breeds responded to these stimuli and showed similarly high MT^1 (AHTMR: WT: 588 mN (range: 147–588 mN) vs. Tac1 KO: 588 (range: 588–980 mN); CHTMR: WT 588 mN (range: 588–980 mN) vs. Tac1 KO: 588 mN (588–980 mN)). AHTMRs were the only afferents that displayed long-lasting PDH as previously described[31] after their initial activation (WT: 6 mV ± 0.2 vs. Tac1 KO: 4 mV ± 0.5). No significant difference was detected between WT and Tac1 KO in other electrical parameters in any of the different subtypes of afferents (Table 1).

Tonic stimulation. In general, WT and Tac1 KO LTMRs responded exclusively and briefly to the initial contact of the clamp and its removal (see below), whereas nociceptive afferents (A and C HTMRs) slowly adapted to this

Table 1. Normal animals' basal somatic cellular electrical properties.

				Normal								
							Active electrical properties					
				Passive electrical properties			Spike				AHP	
	Type	N	CV m/s	Em (mV)	Ri (MΩ)	T (ms)	Amplitude (mV)	D50 (ms)	MDR, (dV/s)	MRR (dV/s)	Amplitude (mV)	AHP50 (ms)
WT	LTMR	14	11 ± 2	−57 ± 2.3	93 ± 16	1.6 ± 0.2	41 ± 2.6	0.8 ± 0.1	86 ± 10	−53 ± 5	7 ± 1	4 ± 0.8
	AHTMR	6	7 ± 1	−57 ± 5.7	137 ± 36	2.4 ± 0.2	56 ± 8.5	1.7 ± 0.2	91 ± 11	−52 ± 21	12 ± 1	12 ± 6.6
	CHTMR	4	0.6 ± 0.2	−58 ± 4.6	210 ± 29	6.3 ± 1.6	66 ± 2.1	3.0 ± 0.3	68 ± 10	−39 ± 5	13 ± 1	14 ± 2.7
Tac1 KO	LTMR	11	11 ± 2	−54 ± 3.4	95 ± 18	1.7 ± 0.1	43 ± 4.9	0.8 ± 0.1	143 ± 20	−55 ± 12	7 ± 2	4 ± 1.3
	AHTMR	8	8 ± 1	−62 ± 4.5	133 ± 23	2.8 ± 0.4	54 ± 5.7	1.2 ± 0.3	111 ± 19	−68 ± 10	19 ± 1	7 ± 1.2
	CHTMR	5	0.6 ± 0.1	−47 ± 1.8	311 ± 39	6.0 ± 0.8	65 ± 5.3	2.5 ± 0.2	91 ± 11	−42 ± 7	19 ± 4	8 ± 1.3

Note: Data are presented as ±standard error. CV: conduction velocity; WT: wild type; Tac1 KO; Tac1 knockout; AHP: after hyperpolarization; LTMR: low-threshold mechanoreceptors; AHTMR: A-fiber high-threshold mechanoreceptor; CHTMR: C-fiber high-threshold mechanoreceptor; MDR: maximum depolarization rate; MRR: minimum repolarization rate.

stimulus. Importantly, nociceptive afferents from WT animals responded for the full duration of the stimulus with three clearly observable stages (rising, falling, and plateau; example of one cell in Figure 2(a)). In contrast, AHTMR afferents from Tac1 KO animals adapted more rapidly than those from normal animals, failing to encode the stimulus duration. In addition, CHTMR responses differed markedly between Tac1 KO and normal animals, the former having a sustained effect at high frequency for over 30 s, followed by rapid failure to respond and marked reduction in membrane potential (Figure 2(b)). Cell population responses are summarized below.

LTMRs: All these afferents responded to tonic stimulation in an on–off manner discharging only to the clamp application and its removal. The on response was brisk with 17.4 ± 3.1 APs in WT and 20.1 ± 2.8 APs in Tac1 KO, and the two breeds did not differ in either IFmax (WT: 169 ± 11 and Tac1 KO: 183 ± 5 Hz) or in time to adaptation (on duration WT: 0.5 ± 0.09 and Tac1 KO: 0.3 ± 0.09 s). Cells from both breeds were also similar in the number of APs on clamp removal (WT: 6.1 ± 1.5 and Tac1 KO: 8.2 ± 2 APs).

HTMRs-WT: All these nociceptive afferents showed a tonic response to the clamp application, discharging during the full duration of the stimulus (120 s). Of these, 6 of the 10 cells (3 AHTMRs and 3 CHTMRs) also developed low-frequency (∼ 0.1 Hz) spontaneous activity after the stimulus that lasted longer than 60 s. However, several differences were observed between these nociceptors. AHTMRs responded with significantly more APs per stimulus (281 ± 67) than CHTMRs (82 ± 21; $p < 0.05$) and with significantly higher IFmax (141 ± 18 Hz) than CHTMRs (29 ± 15 Hz; $p < 0.01$).

RP: This was the shortest phase of cellular response, reaching the IFmax in 0.3 ± 0.1 s in AHTMRs and 0.6 ± 0.1 s in CHTMRs. Although both types of nociceptors discharged a similar number of APs during this phase (AHTMRs: 19 ± 5 vs. CHTMRs 11 ± 2), the IFmean was significantly greater in AHTMRs (82 ± 5 Hz) than in CHTMRs (15 ± 7 Hz; $p < 0.001$).

FP: AHTMR response fell to a plateau faster (1.2 ± 0.3 s) than that of CHTMRs (4 ± 0.9 s; $p < 0.05$). Despite the shorter duration of this phase in AHTMRs, they discharged more APs during this period (57 ± 9) than CHTMRs (19 ± 5; $p < 0.05$) due to a higher IFmean (AHTMR: 72 ± 16 vs. CHTMR: 11 ± 8 Hz; $p < 0.05$).

Plateau response: This phase represented ∼96% of the cellular response (AHTMRs: 118 ± 2; CHTMRs 111 ± 1 s), AHTMRs discharged significantly more APs during this phase (174 ± 34) at a higher IFmean (5.4 ± 0.9 Hz) than CHTMRs (54 ± 15 APs; 1.5 ± 0.9 Hz; $p < 0.05$ for both).

HTMRs-Tac1 KO: None of nociceptive afferents responded through the full 120 s of tonic stimulation, with a similar duration of response (AHTMRs 53 ± 10 s, CHTMRs38 ± 10 s). In contrast to WT nociceptors, AHTMRs from Tac1 KO mice discharged significantly fewer APs than CHTMRs during stimulation (AHTMRs: 180 ± 39 vs. CHTMRs: 833 ± 313; $p < 0.01$) but, like WT, did display a higher IFmax (AHTRMs: 119 ± 24 Hz vs. CHTMRs: 33 ± 1 Hz; $p < 0.05$). This unexpected difference in the pattern of discharge of these afferents was due to changes in the response dynamics and the duration of the RP and FP of their adaptive response to tonic stimulation.

RP: Unlike in WT mice, AHTMRs reached IFmax much quicker than CHTMRs (0.4 ± 0.1 vs. 14 ± 5 s,

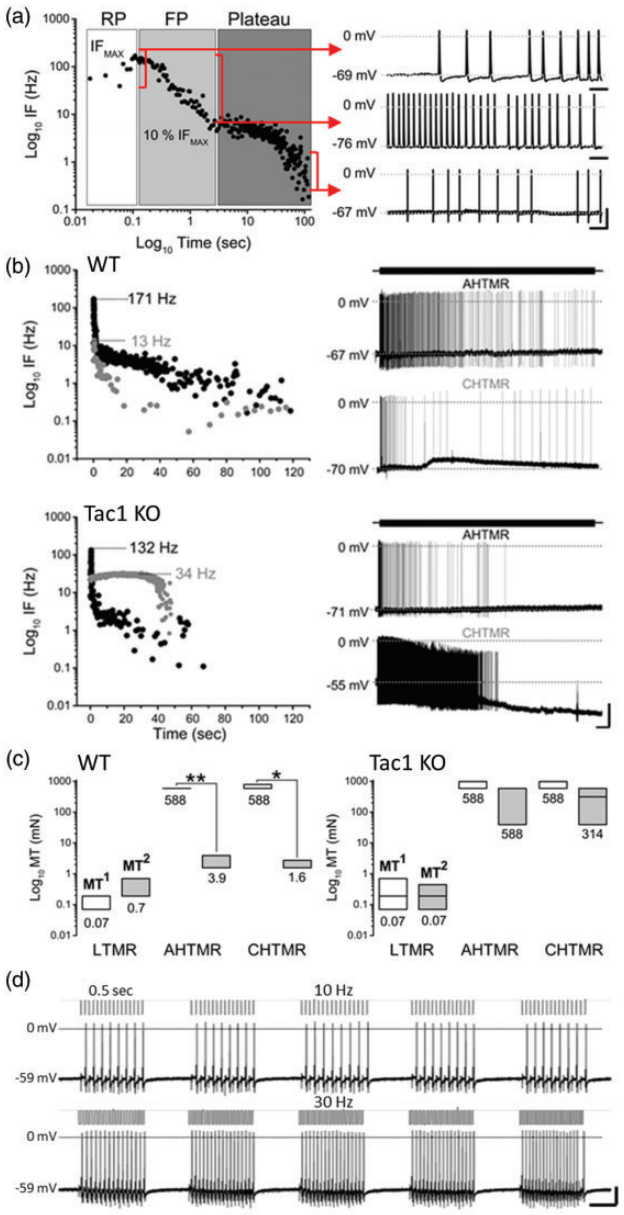

Figure 2. (a) Representative of the performed analysis during the three phases (rising phase (RP), falling phase (FP), and plateau) of the cellular response to tonic mechanical stimulation. Red bracket indicates the area represented in the recording (right, cellular response). IFmax: maximal instantaneous frequency (Hz). Notice the inflection at the end of the FP corresponding with 10% of the IFmax. Scale bars: 0.2 s (RP), 2 s (FP) and 20 s (plateau), respectively, and 20 mV. (b) Representative of the nociceptive response to tonic mechanical stimulation (120 gr, 120 s). Data are presented as IF (left, IF, AHTMR: black, CHTMR: gray) and IFmax values with their actual recorded response (right) during the stimulation (black upper bar). Scale bar: 10 s, 15 mV. (c) Effect of tonic stimulation on the threshold (after (MT^1) and before (MT^2)) of different subtypes of mechanosensitive afferents on control WT and Tac1 KO animals. Data are presented with the location of recorded nociceptive afferents in the L4 dermatome and its proportional distribution per cellular subtype (pie charts) (*$p < 0.05$, **$p < 0.01$). (d) Typical AHTMR response to vibration (10 and 30 Hz (pulse train: 500 ms, 2 Hz)) after tonic stimulation. Scale bars: 200 ms, 20 mV. IF: instantaneous frequency; Tac1 KO; Tac1 knockout; WT: wild type; MT: mechanical threshold; LTMR: low-threshold mechanoreceptors; AHTMR: A-fiber high-threshold mechanoreceptor; CHTMR: C-fiber high-threshold mechanoreceptor.

$p < 0.01$). Also, AHTMRs discharged significantly fewer APs than CHTMRs during this phase (AHTMR: 15 ± 3 vs. 361 ± 182, $p < 0.01$) and demonstrated a significantly lower IFmean than CHTMRs (AHTMR: 49 ± 9 Hz vs. CHTMR: 26 ± 3 Hz; $p < 0.05$), opposite of findings in WT mice.

FP: AHTMRs adapted significantly faster than CHTMRs (AHTMRs: 1.1 ± 0.5 vs. CHTMRs: 18 ± 3.5 s; $p < 0.001$), discharging significantly fewer APs (AHTMRs: 32 ± 10 vs. CHTMRs: 441 ± 112; $p < 0.001$) at higher IFmean (59 ± 14 Hz) than CHTMRs (26 ± 2 Hz; $p < 0.05$).

Plateau response: The duration of this phase was longer for AHTMRs responded (52 ± 10 s) than for CHTMRs (7 ± 0.8 sec; $p < 0.05$), with more APs (AHTMR: 139 ± 31 vs. CHTMR: 33 ± 9; $p < 0.05$) at a lower IFmean (AHTMR: 6 ± 1.1 and CHTMR: 13 ± 1.6 Hz; $p < 0.05$).

Electrical effects of tonic stimulation. As mentioned above, LTMRs responded only to the beginning and end of the tonic stimulus. This limited activation did not modify their electrical properties (Table 2). In contrast, HTMRs responded vigorously to the stimulus and their response significantly modulated some passive and active properties of these afferents in both WT and Tac1 KO animals in a differential and opposite manner depending upon nociceptor subtype as described below.

AHTMRs: At the beginning of their response, AHTMRs from WT and Tac-1KO mice had similar Em and hyperpolarized after activation (PDH), WT: 6 ± 0.2 vs. Tac1 KO: 4 ± 0.5 mV). However, in WT animals, PDH of AHTMRs rapidly disappeared ($\sim$ 10 s) and its Em depolarized. In contrast, AHTMRs from Tac1 mice KO continued to display PDH (mean value of 6 ± 1.5 mV) throughout the duration of the tonic stimulus. Although Em was similar at the beginning of the stimulus, it differed between breeds by the end of the response (WT: -50 ± 5 mV vs. Tac1 KO: -68 ± 6 mV; $p < 0.05$). No other significant differences in the active properties of these afferents were observed after its activation.

CHTMRs: These nociceptive afferents did not display PDH. CHTMRs from WT mice displayed a significantly lower Em than CHTMRs from KO mice (WT: -58 ± 4.6 mV vs. Tac1 KO: -47 ± 1.8 mV; $p < 0.05$). Two of the four CHTMRs from WT mice showed a transient depolarization with return to prestimulus values (Figure 2(b);

Table 2. Effect of paw incision on somatic cellular electrical properties.

				Paw incision								
							Active electrical properties					
				Passive electrical properties			Spike				AHP	
	Type	N	CV m/s	Em (mV)	Ri (MΩ)	T (ms)	Amplitude (mV)	D50 (ms)	MDR (dV/s)	MRR (dV/s)	Amplitude (mV)	AHP50 (ms)
WT	LTMR	6	15 ± 3	−62 ± 6.3	70 ± 3	1.6 ± 0.2	38 ± 2.2	0.8 ± 0.1	121 ± 33	−50 ± 7	5 ± 2	3 ± 1.5
	AHTMR	9	7 ± 2	−52 ± 3.5	146 ± 31	2.7 ± 0.3	55 ± 5.7	1.7 ± 0.2	81 ± 14	−49 ± 8	16 ± 3	10 ± 2.2
	CHTMR	4	0.6 ± 0.2	−46 ± 2.3	299 ± 60	4.9 ± 0.9	62 ± 4.1	2.1 ± 0.2	93 ± 19	−45 ± 7	16 ± 5	9 ± 2.1
Tac1 KO	LTMR	11	12 ± 5	−59 ± 3.5	88 ± 3	1.4 ± 0.3	34 ± 3.3	0.9 ± 0.2	115 ± 16	−53 ± 8	9 ± 2	4 ± 0.8
	AHTMR	5	9 ± 2	−50 ± 1.8	103 ± 34	2.2 ± 0.4	66 ± 4.6	1.9 ± 0.3	105 ± 22	−55 ± 7	17 ± 5	8 ± 3.1
	CHTMR	2[a]	0.7 ± 0.1	−44 ± 0.5	245 ± 39	5.1 ± 2.9	69 ± 5.5	1.6 ± 0.4	88 ± 36	−49 ± 17	17 ± 1	6 ± 1.5

Note: Data are presented as ±standard error. CV: conduction velocity; WT: wild type; Tac1 KO; Tac1 knockout; AHP: after hyperpolarization; LTMR: low-threshold mechanoreceptors; AHTMR: A-fiber high-threshold mechanoreceptor; CHTMR: C-fiber high-threshold mechanoreceptor; MDR: maximum depolarization rate; MRR: minimum repolarization rate.
[a]Tac1 KO CHTMR (too few data points for Shapiro–Wilk).

mean Em −60 ± 3.6 mV). Tonic stimulation resulted in reduced D50 of CHTMRs (from 3 ± 0.3 to 1.1 ± 0.2 ms; $p < 0.01$) but no change in AP amplitude (from 66 ± 2.1 to 57 ± 3.3 mV). Kinetics of APs (MDR: maximum depolarization rate and MRR: minimum repolarization rate (dmV/s)) and the AHP amplitude or duration were not altered by tonic stimulation in WT mice.

CHTMRs from Tac1 KO mice responded in a markedly different manner than that of WT mice. All Tac1 KO CHTMR afferents exhibited a slow prolonged and significant hyperpolarization during tonic stimulation (from −47 ± 1.8 mV to −59 ± 2 mV; $p < 0.01$) that continued even after the cell stopped its discharge. In the final phase of their response, CHTMR afferents showed a significant reduction in AP amplitude from 65 to 47 mV (± 3.2 mV) ($p < 0.05$) without change in AP duration (D50) from 2.5 ± 0.2 to 3.5 ± 0.4 ms but reduced MDR (from 91 ± 11 to 46 ± 8 dV/s ($p < 0.05$) and MDD from −42 ± 7 to −22 ± 3 dV/s ($p < 0.05$). AHP amplitude and duration were not altered by tonic stimulation.

Mechanical sensitization. Afferents within each recorded from WT and Tac1 KO mice had similar initial MT (MT^1). HTMR afferents were collected mostly innervating hairy skin within the L4 dermatome. Whereas LTMR afferents responded to early tactile stimulation (brushing, TF, and 10 Hz vibration), none of the HTMR afferents from WT or Tac1 KO were initially activated by these stimuli. Both AHTMRs and CHTMRs were significantly sensitized in WT mice after this tonic suprathreshold stimulation as evidenced by a reduced MT^2 (Figure 2(c)). Furthermore, AHTMR and CHTMR afferents were also activated by brushing, but only AHTMR afferents responded to vibratory stimulation within the 10–40 Hz range in WT mice (Figure 2(d)). Higher frequency stimulation only elicited an ON response at the first vibratory pulse. Conversely, in Tac1 KO mice, HTMR afferents were insensitive to mechanical stimulation for a few minutes (1.5–2.5 min) following tonic suprathreshold stimulation. Then, their mechanical threshold returned to prestimulus values (Figure 2(c)). They remained unresponsive to brushing or vibration.

Paw incision

Paw withdrawal threshold and edema. No mice of either breed demonstrated overt behavior indicative of distress.

Paw circumference prior to surgery did not differ between WT and Tac1 KO mice. Paw circumference significantly increased in WT mice 24 h after paw incision, whereas it did not change significantly in Tac KO mice 24 h after surgery (Figure 3(a), upper panel).

Baseline paw withdrawal thresholds were significantly higher in WT mice than in Tac KO mice (Figure 3(a), middle). Both breeds showed a significant reduction in mechanical withdrawal threshold 24 h after paw incision (Figure 3(a), middle).

Baseline weight bearing hindpaw distribution was symmetric and similar in both mouse breeds (Figure 3(a), bottom). Paw incision induced asymmetry in weight bearing in both breeds, although the groups differed at both 3 and 24 h after incision (Figure 3(a), bottom).

Electrophysiology

Dynamics of cellular response and MT. All LTMR afferents showed a phasic (on–off) response to punctate stimulation and responded to brushing and the application of the 256 Hz TF with high fidelity (1:1). The MTs of LTMRs from WT mice were significantly higher than those from

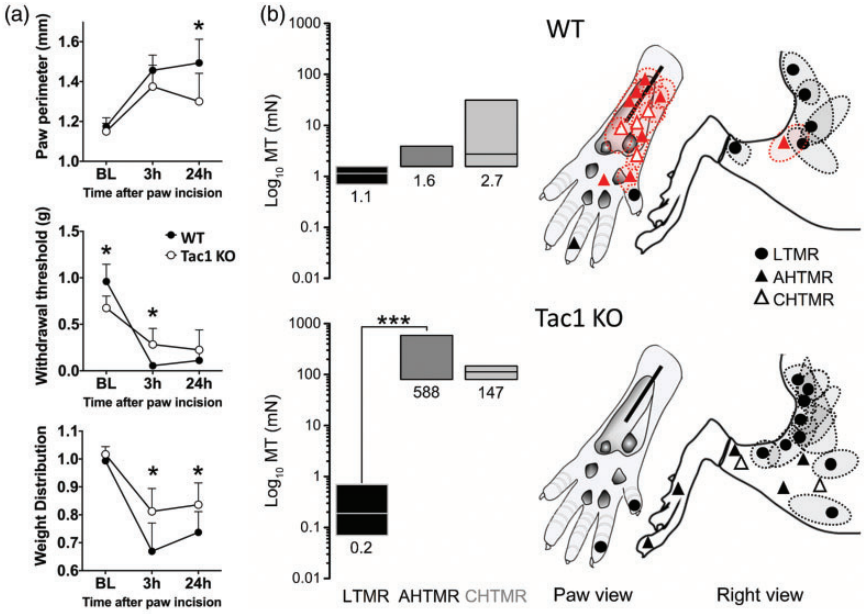

Figure 3. (a) Quantification of paw circumference (upper), 50% paw withdrawal threshold (middle), and hind paw weight bearing distribution (bottom) before and after paw incision (3 h and 24 h) in WT and Tac1 KO mice. (b) Effect of paw incision in the threshold (MT, left) of different subtypes of mechanosensitive afferents. Data were obtained by intracellular recording in the same animals followed its behavioral study. Data are presented with the location (●: LTMR; ▲: AHTMR; Δ: CHTMR) and approximate size of the cellular RF (dotted line) of recorded afferents in the L4 dermatome (glabrous and hairy skin). Sensitized nociceptive afferents of both types (a and c) are presented in red. Notice the absence of nociceptive afferents innervating the incision area in Tac1 KO animals. Presented MT of Tac1 KO nociceptive afferents were obtained in other areas within the L4 dermatome. ***$p < 0.001$, **$p < 0.01$, *$p < 0.05$. Tac1 KO; Tac1 knockout; WT: wild type; MT: mechanical threshold; LTMR: low-threshold mechanoreceptors; AHTMR: A-fiber high-threshold mechanoreceptor; CHTMR: C-fiber high-threshold mechanoreceptor; BL: baseline.

Tac1 KO mice (WT: 1.1 mN (range: 0.7–3.9 mN) vs. Tac1 KO: 0.19 mN (0.07–1.75 mN); $p < 0.05$).

In contrast to LTMRs, all HTMRs showed a tonic response and were incapable of following the 256 Hz TF stimulus. WT nociceptive afferents were significantly sensitized after incision, as witnessed by lower MT than Tac1 KO nociceptors (1.57 mN (range: 0.7–58.8 mN) vs. 147 mN (range: 80–588 mN); $p < 0.001$) (Figure 3(b)). None of these sensitized WT nociceptors showed PDH during threshold activation, whereas four of the seven Tac1 KO nociceptors (all AHTMRs) sharply hyperpolarized after activation (7.5 mV (range: 6–10 mV)). Approximately half of the sensitized nociceptors from WT mice responded to brushing (four of the nine AHTMRs and two of the four CHTMRs). Paw incision did not modify the electrical signature of the afferents across different modalities between WT and Tac1 KO animals compared to nonsurgical animals (Table 2).

Although the likelihood of impaling cells with a mechanosensitive RF was similar after paw incision (WT: 65% vs. Tac1 KO: 68%), most nociceptive afferents from WT mice (12 of the 13) innervated the area near the surgical wound, whereas no nociceptive afferents were identified in the proximity of the wound area of Tac1 KO (Figure 3(b), right panel).

Electrical properties

CHTMRs from WT mice displayed a significantly more depolarized Em (-46 ± 2.3 mV) following paw incision when compared to naive mice (-58 ± 4.6 mV, $p < 0.05$). AHTMRs from Tac1 KO mice displayed a significantly more depolarized Em (-50 ± 1.8 mV) following paw incision when compared to naive Tac1 KO mice (62 ± 4.5 mV; $p < 0.05$).

Immunocytochemistry

Following electrophysiological characterization, L4 ganglia (contralateral and ipsilateral to surgery) were extracted from both four WT and four Tac1 KO animals. Immunoreactivity to SP, CGRP, and TRPV1 were analyzed from WT and Tac1 KO mice in 119 and 43 cells ipsilateral and 85 and 39 cells contralateral to surgery, respectively. Only cells that were positive to at least one of the analyzed molecules were included.

L4 ganglia immunoreactivity contralateral to incision. SP-WT: SP immunoreactivity was present in in 44 of the 85 cells, widely distributed among small to large diameter cells (median: 25 μm (range: 12–46 μm)). Most of these cells (26 cells, ~60%) were only reactive to SP, whereas some costained for CGRP, TRPV1, or both (Figure 4

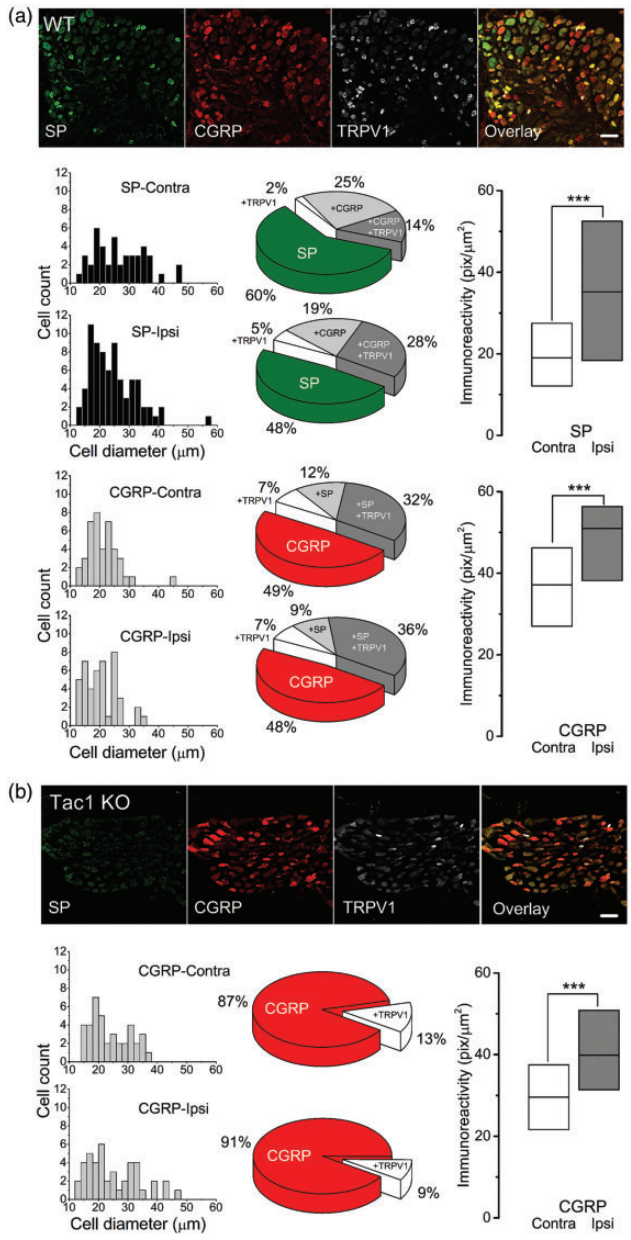

Figure 4. Representative SP (green), CGRP (red), TRPV1 (white), and their overlay immunoreactivity in sections of L4 dorsal root ganglia visualized by confocal microscopy. Data (contra and ipsilateral) are presented with the cell count per cell diameter (bin 2, μm) (left column), proportional distribution (pie charts, middle column), and overall immunoreactivity (pixel/area (pix/μm^2)) (right column) for both WT (a) and Tac1 KO (b), 24 h after paw incision. ***$p < 0.001$. Scale bar: 50 μm. CGRP: calcitonin gene-related peptide; TRPV1: transient receptor potential cation channel vanilloid 1; SP: substance P; Tac1 KO; Tac1 knockout.

(a)). Although there was no difference in the diameter of single- or double-positive cells (median: 27 μm (range: 12–46 μm), the triple-positive population was restricted to a significantly smaller diameter cells (median: 17 μm (range: 15–29 μm); $p < 0.05$). *SP-Tac1 KO*: As expected, there were no SP immuno-positive cells in tissue from these animals. *CGRP-WT*: CGRP immunoreactivity was observed in 41 of the 85 cells with broadly distributed diameter (median: 20 μm (range: 13–45 μm)). As with SP, approximately 50% of the population was only reactive to CGRP with the remainder coexpressing SP alone or with TRPV1 (Figure 4(a)). *CGRP-Tac1 KO*: Most of these cells (87% (34 of the 39)) were only reactive for CGRP with the remainder also positive for TRPV1 (Figure 4(b)).

L4 ganglia immunoreactivity ipsilateral to incision. *SP-WT*: SP immunoreactivity was present in 75 of the 119 cells that were positive for SP after paw incision. There was an increase in immunoreactivity density after surgery as measured by number of pixels above a fixed threshold ipsilateral compared to contralateral to surgery (37.1 ± 2.3 vs. 21.9 ± 2.6 pix/μm^2, respectively, $p < 0.001$). There were no differences in the diameter of immuno-positive cells after paw incision or in the proportion with multiple labeling (Figure 4(a)). *CGRP-WT*: CGRP immunoreactivity was present in 44 of the 85 after paw incision. As SP, there was an increase in CGRP immunoreactivity staining density after surgery as measured by the number of pixels above a fixed threshold ipsilateral compared to contralateral to paw incision surgery (48.8 ± 1.8 pix/μm^2 vs. 37.9 ± 2.3 pix/μm^2; $p < 0.001$). Surgery did not alter the proportion of CGRP immuno-positive cells alone or colocalized with other markers or of the diameter of positive cells (Figure 4(a)). *CGRP-Tac1 KO*: CGRP immunoreactivity was increased ipsilateral compared to contralateral to paw incision surgery (40.5 ± 1.8 pix/μm^2 vs. 29.8 ± 1.6 pix/μm^2; $p < 0.001$) without a difference in proportion of single- to double-labeled cells or cell diameter (Figure 4(b)).

Discussion

Tachykinins are classically thought to drive neurotransmission, encode pain intensity, and participate in central sensitization through actions in the central nervous system. This study uncovers profound effects on peripheral sensitization from sustained activation and injury when tachykinins are missing, suggesting that peripheral actions may be just as important. The principal observations of our studies are that lack of tachykinins (1) prevents nociceptors from properly encoding the duration and magnitude of a sustained nociceptive stimulus, (2) prevents nociceptors from properly encoding peripheral nociceptive sensitization following peripheral damage; and (3) does not results in downregulation of other factors that are relevant to peripheral nociceptive sensitization (i.e., CGRP and TRPV1).

Together, our observations indicate a pivotal role of tachykinins in the overall control of peripheral cellular nociceptive excitability and that of nociceptive activation to trigger this change. Our results also suggest that the development of peripheral mechanical sensitization cannot be explained by the actions of a single factor (e.g., CGRP).

Technical considerations

The inability to tightly control a sustained mechanical stimulus, as discussed by Boada et al.,[31] greatly limits our ability to examine the dynamics of the sensitization process of these afferents. Although this study partially resolved this limitation, the amount and speed of the force that is applied to the nociceptive terminal via a calibrated clamp on the skin remains a function of the tissue composition, thickness, tenso-elastic properties, and terminal peripheral architecture. It is conceivable that difference between these parameters in different breeds of mice may modulate the dynamics of the cellular response to activation. This would not, however, explain the sudden failure of the Tac1 KO nociceptors or the absence of mechanical sensitization after activation.

Tac1 KO nociceptive response to tonic mechanical activation

Although the electrical signature of nociceptive afferents is identical in Tac1 KO as WT mice, some specific components of the transductional mechanism of mechano-nociceptive response are either disrupted or entirely missing in the animals lacking tachykinins.

While the initial dynamic component (RP/FP) was still present on both A and C nociceptive afferents, the static (phase) of the normal adaptive response to a sustained stimulus in different species[27,35] has been lost on the transgenic animals. Furthermore, the CHTMR response to a sustained noxious mechanical stimulus was greatly distorted and transiently amplified.

Nociceptors are activated by mechanical stimuli through stimulation of specific mechanosensitive channels,[36] and the relation between different expression of mechanosensitive channels in DRG neurons and their response has been studied in vitro with some detail.[37–41] Importantly, it has been observed that mechanosensitive channel gating in sensory neurons depends on both the force exerted and the sensitivity to that force,[42] leading to activity decay with tonic stimulation. This process (mechanosensitive channel relaxation) is voltage-dependent, more pronounced at negative membrane potential values[42] and Ca^{2+} dependent.[43,44] Given that tachykinins induce of inward currents[45–48] leading to cellular depolarization,[49–52] tachykinins (particularly SP) may modulate nociceptor responsiveness by controlling the cellular membrane potential during the activation of the terminal. Although this could explain the sudden brake on nociceptor response when tachykinins are missing in the Tac1 KO mouse, it does not address the distorted activation of the CHTMR subtype with sustained stimulation.

Nociceptive sensitization after tonic stimulation

Although early work suggested that mechanical sensitization is not associated with a significant reduction in nociceptor thresholds,[53] later work has shown that suprathreshold mechanical activation sensitizes both A and C nociceptive afferents.[35] This effect is greater on A than C nociceptors and is limited to the dynamic (initial) phase of the response. Our results clearly concur with this classical observation and extend this description also to mice, showing profound sensitization, particularly of AHTMRs, reaching thresholds typical of tactile afferents. This sensitization process is so marked that both A- and C-nociceptors begin to react to tactile stimulation (brushing) and in some cases (AHTMR) even to vibration.

In this context, several manuscripts define allodynia as a pain sensation generated by physiological stimulation of LTMRs, while pain generated by physiologically sensitized nociceptors is defined as hyperalgesia (for review see Jänig[54]). The failure into inducing a change in the mechanical threshold of nociceptive afferents in animal models[53,55] and the observation that activation of mechanosensitive large diameter myelinated, and unmyelinated tactile afferents elicits pain in humans,[56–59] have supported these definitions. Our results show that these definitions need to be revised when applied to rodents in that clear sensitization of high-threshold mechanoreceptors, which occurs after a variety of injuries,[22,31,60–62] is grossly disrupted in the absence of tachykinins.

Despite this deep sensitization process generated by the activation of both types of nociceptive afferents, neither of them showed discharge patterns that fit the sensory events (increased pain perception) as described in classical human psychophysical experiments using prolonged noxious mechanical stimulation.[63] While A-nociceptors shows a more robust response that C-nociceptors, these afferents still adapt during stimulation. Although speculative, the failure of both mechanosensitive nociceptive afferents to correlate with the pain sensation indicates the existence of an amplification mechanism (long-lasting excitation and long after-discharges) at some point in the signal integration process, likely at the superficial dorsal horn. The experimental verification of this speculation is not trivial and will require the use of similar stimulation protocols while recording intracellularly in vivo from secondary order neurons at the superficial dorsal horn

(lamina I and II) connected to both types of mechanonociceptive afferents.

Behavioral changes and neurogenic-related mediators in Tac1 KO mice

Tac1 KO mice have shown to develop a less intense mechanical allodynia than WT mice following paw incision,[64] which is in accordance with our behavioral studies. These findings could be explained by a lack of tachykinin-dependent neurogenic inflammation, as evidenced by reduced paw edema in Tac1 KO mice 24 h after paw incision .Since we also observed an increase in CGRP and TRPV1 expression in DRG neurons following paw incision in the Tac1 KO mice similar to the WT controls, these results indicate that tachykinins are an essential component of the factors responsible for paw edema and behavioral hypersensitivity following paw incision.

We expected to find a diminished responsiveness of nociceptors due to the absence of neurogenic inflammation in Tac1 KO mice. Although normal nociceptive afferents (A and C-HTMR) were easily detectable around the incision area and clearly hyperexcitable,[60,65,66] none were found in Tac1 KO animals. This result was unexpected based on several manuscripts indicating a mild C-fiber modality specific effects of the lack of SP[5,6,67] which suggest that although less sensitive, the nociceptive afferents should be still detectable. This surprising observation suggested that injury might paradoxically reduce nociceptor responsiveness near the site of sustained stimulation, leading us to test application of controlled mechanical noxious stimulus to produce a tonic activation of nociceptors in the absence of injury.

While it is plausible that this failure on detecting these afferents around the wounded area in Tac1 KO may due to the low probability of successful impalement of nonsensitize nociceptive afferents, the analysis of these afferents normal response to activation suggested the presence of two different excitable states on Tac1 KO nociceptive afferents after injury: One nonsensitized state that render these afferents detection highly improbable and a second, a desensitized state reached after activation that blockade the afferent discharge making its detection by all-natural stimulation, extremely difficult.

These results offer an alternative hypothesis to the existing and accepted mechanisms of tachykinins in pain modulation (spinal and supra spinal actions of peripheral afferent release of tachykinins,[5,6] impaired diffuse noxious inhibitory control,[68] diminished inflammatory response[69]). In fact, our findings could explain the origin of these putative central mechanisms of tachykinins. Since primary sensory neurons express tachykinin receptors,[70–72] our results could also be explained by an autocrine effect of tachykinins in primary afferents.

Even though primary sensory neurons not only synthetize tachykinins but also express their cognate receptors,[70–72] all the abovementioned behavioral studies have failed to provide evidence that the primary sensory neurons of these transgenic animals are competent to appropriately encode nociceptive mechanical stimulation. It is surprising that after 20 years since its development none of the studies have aim this important factor that potentially could compromise the interpretability of any study aiming exclusively the central component of the nociceptive sensitization process and pain transmission.

Conclusions

These results suggest that tachykinins are indeed required for the appropriate development of peripheral sensitization and that tachykinins control the membrane electrical excitability of nociceptors and their absence will induce cellular membrane failure to convey the signal generated by the terminal depolarization. Although the central sensitization processes may also be relevant, the failure of these afferent to appropriately transduce the stimuli may adequately explain many behavioral and central neurophysiologic phenomena. Peripheral actions of tachykinins on sensory afferents themselves should be taken in consideration to guide further studies addressing the role of these peptides and their interactions on the development of neuropathic states. Additional studies of the circuitry of the spinal cord of these animals are required to understand the differential contribution of peripheral versus central sensitization in the context of peripheral tissue damage.

Author Contributions

MDB and EAR conceptualized and designed the research; MDB, SG, PAA, and EAR performed the experiments. MDB, SG, and EAR analyzed the data; MDB, SG, and EAR interpreted the results of experiments; MDB prepared the figures; MDB drafted the manuscript; MDB, SG, JCE, and EAR edited and revised the manuscript; MDB, JCE, SG, PAA, and EAR approved the final version of manuscript.

Declaration of Conflicting Interests

The author(s) declared no potential conflicts of interest with respect to the research, authorship, and/or publication of this article.

Funding

The author(s) disclosed receipt of the following financial support for the research, authorship, and/or publication of this article: This work was supported by grant R37-GM48085 (James C. Eisenach) from the National Institutes of Health.

ORCID iD

M Danilo Boada https://orcid.org/0000-0002-8973-3010

References

1. Harlan RE, Garcia MM and Krause JE. Cellular localization of substance P- and neurokinin A-encoding preprotachykinin mRNA in the female rat brain. *J Comp Neurol* 1989; 287: 179–212.
2. Krause JE, Chirgwin JM, Carter MS, Xu ZS and Hershey AD. Three rat preprotachykinin mRNAs encode the neuropeptides substance P and neurokinin A. *Proc Natl Acad Sci U S A* 1987; 84: 881–885.
3. Otsuka M and Yoshioka K. Neurotransmitter functions of mammalian tachykinins. *Physiol Rev* 1993; 73: 229–308.
4. Borbely E, Hajna Z, Sandor K, Kereskai L, Toth I, Pinter E, Nagy P, Szolcsanyi J, Quinn J, Zimmer A and Stewart J. Role of tachykinin 1 and 4 gene-derived neuropeptides and the neurokinin 1 receptor in adjuvant-induced chronic arthritis of the mouse. *PLoS One* 2013; 8: e61684–e61604.
5. Cao YQ, Mantyh PW, Carlson EJ, Gillespie A-M, Epstein CJ and Basbaum AI. Primary afferent tachykinins are required to experience moderate to intense pain. *Nature* 1998; 392: 390–394.
6. Zimmer A, Zimmer AM, Baffi J, Usdin T, Reynolds K, König M, Palkovits M and Mezey E. Hypoalgesia in mice with a targeted deletion of the tachykinin 1 gene. *Proc Natl Acad Sci U S A* 1998; 95: 2630–2635.
7. Felipe CD, Herrero JF, O'Brien JA, Palmer JA, Doyle CA, Smith AJH, Laird JMA, Belmonte C, Cervero F and Hunt SP. Altered nociception, analgesia and aggression in mice lacking the receptor for substance P. *Nature* 1998; 392: 394–397.
8. Duggan AW, Morton CR, Zhao ZQ and Hendry IA. Noxious heating of the skin releases immunoreactive substance P in the substantia gelatinosa of the cat: a study with antibody microprobes. *Brain Res* 1987; 403: 345–349.
9. Hill R. NK1 (substance P) receptor antagonists–why are they not analgesic in humans? *Trends Pharmacol Sci* 2000; 21: 244–246.
10. Iliff JJ, Fairbanks SL, Balkowiec A and Alkayed NJ. Epoxyeicosatrienoic acids are endogenous regulators of vasoactive neuropeptide release from trigeminal ganglion neurons. *J Neurochem* 2010; 115: 1530–1542.
11. Guo TZ, Wei T, Shi X, Li WW, Hou S, Wang L, Tsujikawa K, Rice KC, Cheng K, Clark DJ and Kingery WS. Neuropeptide deficient mice have attenuated nociceptive, vascular, and inflammatory changes in a tibia fracture model of complex regional pain syndrome. *Mol Pain* 2012; 8: 85.
12. Weinstock JV, Blum A, Metwali A, Elliott D, Bunnett N and Arsenescu R. Substance P regulates Th1-type colitis in IL-10 knockout mice. *J Immunol* 2003; 171: 3762–3767.
13. Botz B, Imreh A, Sándor K, Elekes K, Szolcsányi J, Reglődi D, Quinn JP, Stewart J, Zimmer A, Hashimoto H and Helyes Z. Role of pituitary adenylate-cyclase activating polypeptide and Tac1 gene derived tachykinins in sensory, motor and vascular functions under normal and neuropathic conditions. *Peptides* 2013; 43: 105–112.
14. Barabas ME and Stucky CL. TRPV1, but not TRPA1, in primary sensory neurons contributes to cutaneous incision-mediated hypersensitivity. *Mol Pain* 2013; 9: 9.
15. Jang JH, Nam TS, Paik KS, Leem JW. Involvement of peripherally released substance P and calcitonin gene-related peptide in mediating mechanical hyperalgesia in a traumatic neuropathy model of the rat. *Neurosci Lett* 2004; 360: 129–132.
16. Nakamura-Craig M and Gill BK. Effect of neurokinin A, substance P and calcitonin gene related peptide in peripheral hyperalgesia in the rat paw. *Neurosci Lett* 1991; 124: 49–51.
17. Guo A, Vulchanova L, Wang J, Li X and Elde R. Immunocytochemical localization of the vanilloid receptor 1 (VR1): relationship to neuropeptides, the P2X3 purinoceptor and IB4 binding sites. *Eur J Neurosci* 1999; 11: 946–958.
18. Zwick M, Davis BM, Woodbury CJ, Burkett JN, Koerber HR, Simpson JF and Albers KM. Glial cell line-derived neurotrophic factor is a survival factor for isolectin B4-positive, but not vanilloid receptor 1-positive, neurons in the mouse. *J Neurosci* 2002; 22: 4057–4065.
19. Sinclair SR, Kane SA, Van der Schueren BJ, Xiao A, Willson KJ, Boyle J, de Lepeleire I, Xu Y, Hickey L, Denney WS, Li C-C, Palcza J, Vanmolkot FHM, DeprÃ© M, Van Hecken A, Murphy MG, Ho TW and de Hoon JN. Inhibition of capsaicin-induced increase in dermal blood flow by the oral CGRP receptor antagonist, telcagepant (MK-0974). *Br J Clin Pharmacol* 2010; 69: 15–22.
20. Szallasi A, Cruz F and Geppetti P. TRPV1: a therapeutic target for novel analgesic drugs? *Trends Mol Med* 2006; 12: 545–554.
21. Takasusuki T and Yaksh TL. Regulation of spinal substance p release by intrathecal calcium channel blockade. *Anesthesiology* 2011; 115: 153–164.
22. Boada MD, Houle TT, Eisenach JC and Ririe DG. Differing neurophysiologic mechanosensory input from glabrous and hairy skin in juvenile rats. *J Neurophysiol* 2010; 104: 3568–3575.
23. Boada MD, Gutierrez S, Aschenbrenner CA, Houle TT, Hayashida K-I, Ririe DG and Eisenach JC. Nerve injury induces a new profile of tactile and mechanical nociceptor input from undamaged peripheral afferents. *J Neurophysiol* 2014; 113: 100–109.
24. Boada MD and Woodbury CJ. Physiological properties of mouse skin sensory neurons recorded intracellularly in vivo: temperature effects on somal membrane properties. *J Neurophysiol* 2007; 98: 668–680.
25. Boada MD and Woodbury CJ. Myelinated skin sensory neurons project extensively throughout adult mouse substantia gelatinosa. *J Neurosci* 2008; 28: 2006–2014.
26. Garell PC, McGillis SL and Greenspan JD. Mechanical response properties of nociceptors innervating feline hairy skin. *J Neurophysiol* 1996; 75: 1177–1189.
27. Slugg RM, Meyer RA and Campbell JN. Response of cutaneous A- and C-fiber nociceptors in the monkey to controlled-force stimuli. *J Neurophysiol* 2000; 83: 2179–2191.

28. Cabanes C, López de Armentia M, Viana F and Belmonte C. Postnatal changes in membrane properties of mice trigeminal ganglion neurons. *J Neurophysiol* 2002; 87: 2398–2407.
29. Gallego R and Eyzaguirre C. Membrane and action potential characteristics of A and C nodose ganglion cells studied in whole ganglia and in tissue slices. *J Neurophysiol* 1978; 41: 1217–1232.
30. Yoshida S and Matsuda Y. Studies on sensory neurons of the mouse with intracellular-recording and horseradish peroxidase-injection techniques. *J Neurophysiol* 1979; 42: 1134–1145.
31. Boada MD, Ririe DG and Eisenach JC. Post-discharge hyperpolarization is an endogenous modulatory factor limiting input from fast-conducting nociceptors (AHTMRs). *Mol Pain* 2017; 13: 08–22.
32. Pogatzki EM and Raja SN. A mouse model of incisional pain. *Anesthesiology* 2003; 99: 1023–1027.
33. Saha M, Skopelja S, Martinez E, Alvarez DL, Liponis BS and Romero-Sandoval EA. Spinal mitogen-activated protein kinase phosphatase-3 (MKP-3) is necessary for the normal resolution of mechanical allodynia in a mouse model of acute postoperative pain. *J Neurosci* 2013; 33: 17182–17187.
34. Jimenez-Andrade JM, Mantyh WG, Bloom AP, Xu H, Ferng AS, Dussor G, Vanderah TW and Mantyh PW. A phenotypically restricted set of primary afferent nerve fibers innervate the bone versus skin: therapeutic opportunity for treating skeletal pain. *Bone* 2010; 46: 306–313.
35. Andrew D and Greenspan JD. Mechanical and heat sensitization of cutaneous nociceptors after peripheral inflammation in the rat. *J Neurophysiol* 1999; 82: 2649–2656.
36. Lumpkin EA and Caterina MJ. Mechanisms of sensory transduction in the skin. *Nature* 2007; 445: 858–865.
37. Coste B, Crest M and Delmas P. Pharmacological dissection and distribution of NaN/Nav1.9, T-type Ca2+ currents, and mechanically activated cation currents in different populations of DRG neurons. *J Gen Physiol* 2007; 129: 57–77.
38. Drew LJ, Rugiero F, Cesare P, Gale JE, Abrahamsen B, Bowden S, Heinzmann S, Robinson M, Brust A, Colless B, Lewis RJ and Wood JN. High-threshold mechanosensitive ion channels blocked by a novel conopeptide mediate pressure-evoked pain. *PLoS One* 2007; 2: e515.
39. Drew LJ, Wood JN and Cesare P. Distinct mechanosensitive properties of capsaicin-sensitive and -insensitive sensory neurons. *J Neurosci* 2002; 22: RC228–RC206.
40. McCarter GC and Levine JD. Ionic basis of a mechanotransduction current in adult rat dorsal root ganglion neurons. *Mol Pain* 2006; 2: 28.
41. McCarter GC, Reichling DB and Levine JD. Mechanical transduction by rat dorsal root ganglion neurons in vitro. *Neurosci Lett* 1999; 273: 179–182.
42. Hao J and Delmas P. Multiple desensitization mechanisms of mechanotransducer channels shape firing of mechanosensory neurons. *J Neurosci* 2010; 30: 13384–13395.
43. Crawford AC, Evans MG and Fettiplace R. Activation and adaptation of transducer currents in turtle hair cells. *J Physiol (Lond)* 1989; 419: 405–434.
44. Martinac B. Mechanosensitive ion channels: molecules of mechanotransduction. *J Cell Sci* 2004; 117: 2449–2460.
45. Ishimatsu M. Substance P produces an inward current by suppressing voltage-dependent and -independent K+ currents in bullfrog primary afferent neurons. *Neurosci Res* 1994; 19: 9–20.
46. Paul K and Cox CL. Excitatory actions of substance P in the rat lateral posterior nucleus. *Eur J Neurosci* 2010; 31: 1–13.
47. Shen KZ and North RA. Substance P opens cation channels and closes potassium channels in rat locus coeruleus neurons. *Neuroscience* 1992; 50: 345–353.
48. Soejima T, Endoh T and Suzuki T. Substance P-induced depolarization accompanied by a decrease in membrane input resistance in the hamster submandibular ganglion cell. *Bull Tokyo Dent Coll* 1998; 39: 119–122.
49. Moraes ER, Kushmerick C and Naves LA. Characteristics of dorsal root ganglia neurons sensitive to substance P. *Mol Pain* 2014; 10: 73.
50. Sculptoreanu A, Artim DE and de Groat WC. Neurokinins inhibit low threshold inactivating K+ currents in capsaicin responsive DRG neurons. *Exp Neurol* 2009; 219: 562–573.
51. Takeda M, Tanimoto T, Nasu M, Ikeda M, Kadoi J and Matsumoto S. Activation of NK1 receptor of trigeminal root ganglion via substance P paracrine mechanism contributes to the mechanical allodynia in the temporomandibular joint inflammation in rats. *Pain* 2005; 116: 375–385.
52. Zhang X, Pietra C, Lovati E and de Groat WC. Activation of neurokinin-1 receptors increases the excitability of guinea pig dorsal root ganglion cells. *J Pharmacol Exp Ther* 2012; 343: 44–52.
53. Cooper B, Ahlquist M, Friedman RM and Labanc J. Properties of high-threshold mechanoreceptors in the goat oral mucosa. II. Dynamic and static reactivity in carrageenan-inflamed mucosa. *J Neurophysiol* 1991; 66: 1280–1290.
54. Jänig W. Mechanical allodynia generated by stimulation of unmyelinated afferent nerve fibres. *J Physiol* 2011; 589; 4407–4408.
55. Woolf CJ and McMahon SB. Injury-induced plasticity of the flexor reflex in chronic decerebrate rats. *Neuroscience* 1985; 16: 395–404.
56. Campbell JN, Raja SN, Meyer RA and Mackinnon SE. Myelinated afferents signal the hyperalgesia associated with nerve injury. *Pain* 1988; 32: 89–94.
57. Liljencrantz J, Björnsdotter M, Morrison I, Bergstrand S, Ceko M, Seminowicz DA, Cole J, Bushnell CM and Olausson H. Altered C-tactile processing in human dynamic tactile allodynia. *Pain* 2013; 154: 227–234.
58. Nagi SS, Rubin TK, Chelvanayagam DK, Macefield VG and Mahns DA. Allodynia mediated by C-tactile afferents in human hairy skin. *J Physiol* 2011; 589: 4065–4075.
59. Torebjork HE, Lundberg LE and LaMotte RH. Central changes in processing of mechanoreceptive input in capsaicin-induced secondary hyperalgesia in humans. *J Physiol* 1992; 448: 765–780.

60. Boada MD, Gutierrez S, Giffear K, Eisenach JC and Ririe DG. Skin incision-induced receptive field responses of mechanosensitive peripheral neurons are developmentally regulated in the rat. *J Neurophysiol* 2012; 108: 1122–1129.
61. Boada DM, Martin TJ, Peters CM, Hayashida K, Harris MH, Houle TT, Boyden ES, Eisenach JC and Ririe DG. Fast-conducting mechanoreceptors contribute to withdrawal behavior in normal and nerve injured rats. *Pain* 2014; 155: 2646–2655.
62. Boada MD, Martin TJ and Ririe DG. Nerve injury induced activation of fast-conducting high threshold mechanoreceptors predicts non-reflexive pain related behavior. *Neurosci Lett* 2016; 632: 44–49.
63. Adriaensen H, Gybels J, Handwerker HO, Van JH. Nociceptor discharges and sensations due to prolonged noxious mechanical stimulation–a paradox. *Hum Neurobiol* 1984; 3: 53–58.
64. Sahbaie P, Shi X, Li X, Liang D, Guo T-Z, Qiao Y, Yeomans DC, Kingery WS and David Clark J. Preprotachykinin-A gene disruption attenuates nociceptive sensitivity after opioid administration and incision by peripheral and spinal mechanisms in mice. *J Pain* 2012; 13: 997–1007.
65. Hamalainen MM, Gebhart GF and Brennan TJ. Acute effect of an incision on mechanosensitive afferents in the plantar rat hindpaw. *J Neurophysiol* 2002; 87: 712–720.
66. Pogatzki EM, Gebhart GF and Brennan TJ. Characterization of Aδ- and C-fibers innervating the plantar rat hindpaw one day after an incision. *J Neurophysiol* 2002; 87: 721–731.
67. Sahbaie P, Shi X, Guo T-Z, Qiao Y, Yeomans DC, Kingery WS and Clark DJ. Role of substance P signaling in enhanced nociceptive sensitization and local cytokine production after incision. *Pain* 2009; 145: 341–349.
68. Bester H, De Felipe C and Hunt SP. The NK1 receptor is essential for the full expression of noxious inhibitory controls in the mouse. *J Neurosci* 2001; 21: 1039–1046.
69. Grant AD, Gerard NP and Brain SD. Evidence of a role for NK1 and CGRP receptors in mediating neurogenic vasodilatation in the mouse ear. *Br J Pharmacol* 2002; 135: 356–362.
70. Scott JR, Muangman P and Gibran NS. Making sense of hypertrophic scar: a role for nerves. *Wound Repair Regen* 2007; 15: S27–S31.
71. Sio SWS, Puthia MK, Lu J, Moochhala S and Bhatia M. The neuropeptide substance P is a critical mediator of burn-induced acute lung injury. *J Immunol*. 2008; 180: 8333–8341.
72. Widgerow AD and Kalaria S. Pain mediators and wound healing–establishing the connection. *Burns* 2012; 38: 951–959.